

Simulation and performance analysis of organic Rankine cycle combined heat and power system

Liu Yulan¹ Cao Zheng¹ Chen Jiufa¹ Xiong Jian²

(¹School of Energy and Environment, Southeast University, Nanjing 210096, China)

(²Lotusland Renewable Energy Holdings Limited, Shanghai 200233, China)

Abstract: To improve the overall thermal efficiency of the organic Rankine cycle (ORC), a simulation study was carried out for a combined heat and power (CHP) system, using the Redlich-Kuang-Soave (RKS) equation of state. In the system, R245fa was selected as the working fluid. A scroll expander was modeled with empirical isentropic expansion efficiency. Plate heat exchangers were selected as the evaporator and the condenser, and detailed heat transfer models were programmed for both one-phase and two-phase regions. Simulations were carried out at seven different heat source temperatures (80, 90, 100, 110, 120, 130, 140 °C) in combination with eight different heat sink temperatures (20, 25, 30, 35, 40, 45, 50, 55 °C). Results show that in the ORC without an internal heat exchanger (IHE), the optimum cycle efficiencies are in the range of 7.0% to 7.3% when the temperature differences between the heat source and heat sink are in the range of 70 to 90 °C. Simulations on CHP reveal that domestic hot water can be produced when the heat sink inlet temperature is higher than 40 °C, and the corresponding exergy efficiency and overall thermal efficiency are 29% to 56% and 87% to 90% higher than those in the non-CHP ORC, respectively. It is found that the IHE has little effect on the improvement of work output and efficiencies for the CHP ORC.

Key words: organic Rankine cycle; combined heat and power; cycle efficiency; exergy efficiency; thermal efficiency

doi: 10.3969/j.issn.1003-7985.2015.04.010

With increasing scarcity of non-renewable energy, the development of new energy and recovery of waste heat is increasingly important. Using a low-temperature heat source to generate power with the ORC is one of the effective ways to solve this problem. So far, much research on ORC systems has been carried out, and the form of heat source can be solar^[1], geothermal^[2], biomass^[3], industrial waste heat^[4] and so on. However, what they are most concerned about is the power efficiency. Madhawa et al.^[2] compared different refrigerants in

the ORC system, such as ammonia, HCFC 123, n-pentane and PF5050, however, the maximum power efficiency is not more than 10%. Li et al.^[5] obtained the highest efficiency of 7.98% in the regenerative ORC with 6 kW power output. Jradi et al.^[6] employed HFE7100 in an ORC system, and the maximum electric power of 500 kW has been generated with a cycle efficiency of 5.7%. Zheng et al.^[7] pointed out that the cycle efficiency is steady between 5% and 6% when the heat source temperature is 90 °C. Pei et al.^[8] designed and manufactured a specific turbine to adapt the ORC system in order to improve cycle efficiency, and obtained a maximum efficiency of 6.8%. In summary, as stated in previously mentioned studies, the present thermal efficiency is relatively low in small-scale ORC systems, both under the theoretical and experimental conditions. This phenomenon may be due to two main reasons: the first is the limitations of the research projects themselves; the second is the application limit of the low-grade heat source, which is only used for output power.

Therefore, to compensate for this inadequacy, the discharged heat is recycled in the condenser for domestic hot water by using the CHP technology, thus improving the overall thermal efficiency and reducing the exergy destruction. According to the civil architecture standard of domestic hot water, the temperature of cooling water at the condenser outlet, T_{ow} , should be set in the range of 50 to 60 °C. In addition, a simulation program is developed in this paper to study the ORC and optimized under different conditions. Therefore, it can provide technical support and a theoretical basis for calculating the overall system, and give guidance to the test bench in future research.

1 System Introduction

1.1 Organic working fluids selection

The selection of low boiling point organic working fluid is important for optimizing the ORC system. Apart from its environmental impacts, the thermophysical property of the working fluid should be considered. Qiu^[9] pointed out that R245fa was one of the best working fluids in small-scale ORC systems by proposing some evaluation standards and methods; Aghahosseini et al.^[10] proved that the performance indicators of the ORC were

Received 2015-03-25.

Biographies: Liu Yulan(1990—), female, graduate; Chen Jiufa (corresponding author), male, doctor, professor, chen.jiufa@126.com.

Foundation item: Special Fund for Industry, University and Research Cooperation (No. 2011DFR61130).

Citation: Liu Yulan, Cao Zheng, Chen Jiufa, et al. Simulation and performance analysis of organic Rankine cycle combined heat and power system[J]. Journal of Southeast University (English Edition), 2015, 31(4): 489–495. [doi:10.3969/j.issn.1003-7985.2015.04.010]

all in the most reasonable range by using R245fa under different conditions; Saleh et al.^[11] pointed out that R245fa should be considered in order to obtain a high thermal efficiency in the reheated cycle. In view of the previous studies, R245fa was chosen in this paper for a small-scale ORC system with a low-temperature heat source.

1.2 Basic ORC system

The schematic diagram of a basic ORC is presented in Figs. 1 and 2. The refrigerant enters the condenser as superheated vapor at state 1 and leaves as subcooled liquid at state 4, and the cooling water will take away the heat, which is rejected during this vapor-liquid phase change process at condensing pressure P_d . Then, the refrigerant enters the pump and is compressed to the evaporating pressure P_e in an isentropic efficiency which is determined by the pump. Then, it enters the evaporator as compressed liquid at state 5 and leaves as superheated vapor at state 8 by absorbing heat from the heat carrier at constant P_e . The superheated vapor enters the expander and expands in an isentropic efficiency which is determined by the expansion ratio, and produces work by rotating the shaft connected to a generator. The pressure and temperature of the vapor drop during this process to the initial state 1. Then the refrigerant reenters the condenser, completing the cycle^[12]. During this cycle, work can be produced in the expansion process, which can be used for

generating electricity. Meanwhile, the cooling water at an appropriate temperature can be obtained by controlling the condensing temperature T_d , thus improving the overall thermal efficiency. Furthermore, instead of water, thermal oil serves as the heat carrier.

1.3 ORC system with IHE

Compared with the basic ORC, the thermal load of the condenser and the cooling load of the evaporator can be reduced by adding a counter-flow IHE between the expander and pump outlet pipes, thus improving thermal efficiency. The subcooled liquid refrigerant (at state 5) absorbs heat from the superheated vapor refrigerant (at state 1) in the IHE, then they leave the IHE at state 5i and 2i, respectively, as illustrated in Figs. 3 and 4.

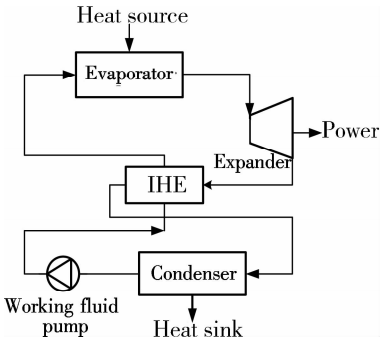


Fig. 3 Schematic diagram of the ORC system with IHE

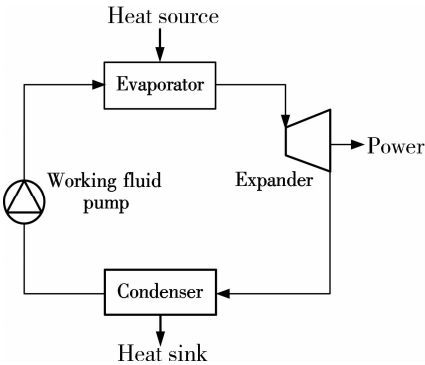


Fig. 1 Schematic diagram of the ORC system

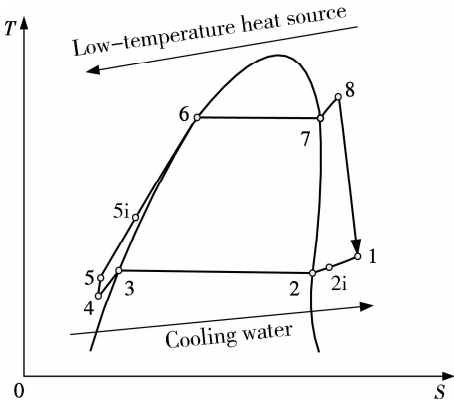


Fig. 4 T-S diagram of the ORC system with IHE

2 ORC Model

A program of the ORC model is developed in this paper, which is written in VB language. The main routine connects the subroutines of working fluid, the evaporator, expander, condenser, pump and IHE. This program is simulated under ideal conditions; i. e., the pressure drops in pipes, heat exchangers and other components are ignored.

2.1 Working fluid subroutine

The physical parameters of R245fa in one-phase and two-phase regions are calculated by using the RKS equa-

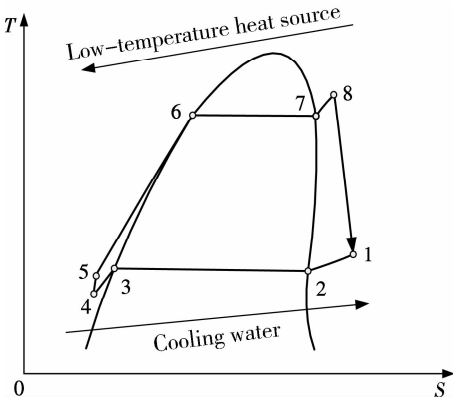


Fig. 2 T-S diagram of the ORC system

tion of state with an elaborated thermodynamic frame. In addition, the following basic parameters are needed: an eccentric factor, molecular weight, critical temperature, critical pressure, the heat capacity of the liquid, and the heat capacity of the ideal gas.

In the superheated or subcooled region, the physical parameters of the working fluid, such as enthalpy, entropy, internal energy, density, can be calculated according to the temperature and pressure. While in the two-phase region, either temperature or pressure is enough for the calculation. For given temperature (or pressure), the fugacity coefficients of both the liquid phase and vapor phase are calculated and compared. If the deviation between those two fugacity coefficients is smaller than a given tolerance, the equilibrium state is reached, and the iterated pressure (or temperature) can be outputted; otherwise, a new iteration process will be repeated. In addition, other physical parameters can be calculated according to the temperature and pressure.

In short, the physical parameters of the working fluid can be calculated in this working fluid subroutine, which provides a basis for the simulation of the entire program.

2.2 Model of evaporator and condenser

The aim of the subroutine of the evaporator model is to output the iterated evaporating temperature T_e , heat exchange Q_e and other outlet parameters. This subroutine is to perform iterative calculation by controlling the deviation between the iterated heat transfer area and the actual area of the evaporator. When the system is equipped with IHE, the heat exchange is

$$Q_e = (h_8 - h_{5i}) q_{m,r} \quad (1)$$

and without IHE, it is

$$Q_e = (h_8 - h_5) q_{m,r} \quad (2)$$

where $q_{m,r}$ is the mass flow rate of refrigerant; h_8 , h_{5i} , h_5 are the enthalpy per unit mass of refrigerant at state 8, 5i, and 5, respectively.

For the chevron plate heat exchanger, the empirical correlation of heat transfer coefficient k in the single-phase region can be calculated as^[13]

$$k = 0.295 \frac{\lambda}{D_{eq}} Re^{0.64} Pr^{0.32} \left(\frac{\pi}{2} - \beta \right)^{0.09} \quad (3)$$

where λ is the thermal conductivity; D_{eq} is the equivalent diameter of the single channel in the plate heat exchanger; Re is the Reynolds number; Pr is the Prandtl number; β is the angle of the herringbone plate heat exchanger.

In the two-phase region, the precise heat transfer coefficient can be calculated as^[14]

$$k = 23.7 k_{il} (75Bo^{0.75} + 0.25Co^{-0.45} Fr_1^{0.25}) \quad (4)$$

where k_{il} is the heat transfer coefficient of the liquid re-

frigerant; Bo is the Boiling number; Co is the convection number; Fr_1 is the Froude number of the liquid refrigerant.

The simulation algorithm of the condenser model is similar to that of the evaporator. In the CHP system, the discharged heat in the condenser is collected for domestic hot water. When the system is equipped with IHE, the discharged heat Q_d is

$$Q_d = (h_{2i} - h_4) q_{m,r} \quad (5)$$

and without IHE, it is

$$Q_d = (h_1 - h_4) q_{m,r} \quad (6)$$

where h_{2i} , h_4 , h_1 are the enthalpy per unit mass of refrigerant at state 2i, 4, and 1, respectively.

The heat transfer coefficient of the two-phase fluid can be calculated as^[13]

$$k = 4.118 \frac{\lambda_1}{D_{eq}} Re_{eq} Pr_1^{0.333} \quad (7)$$

where λ_1 is the thermal conductivity of the liquid refrigerant; Re_{eq} is the equivalent Reynolds number; Pr_1 is the Prandtl number of the liquid refrigerant.

2.3 Model of expander, pump and IHE

For the selected scroll expander, the isentropic efficiency is maximum when the cycle pressure ratio matches the internal volume ratio of the expander, and it will be decreased in over- or under-expansion. The work output W_{exp} is

$$W_{exp} = (h_8 - h_1) q_{m,r} \quad (8)$$

The working fluid pump is used for elevating the pressure of the liquid refrigerant from P_d to P_e , and its simulation algorithm is similar to that of the expander. The power consumption of the pump W_p is

$$W_p = (h_5 - h_4) q_{m,r} \quad (9)$$

In the IHE, the high-pressure liquid refrigerant (at state 5) can be heated by absorbing heat from the low-pressure gas refrigerant (at state 1), and the heat transfer leads to a reduction in the thermal load of the condenser and cooling load of the evaporator, thus improving the cycle efficiency. The heat exchange in the IHE Q_1 is

$$Q_1 = (h_{5i} - h_5) q_{m,r} = (h_1 - h_{2i}) q_{m,r} \quad (10)$$

2.4 Cycle indicators

The net work output W_{net} , cycle efficiency η_{cyc} , exergy efficiency η_{ex} and overall thermal efficiency η_{ove} are set to be the cycle indicators to evaluate the performance of the ORC system and select the optimal working conditions.

$$W_{net} = W_{exp} - W_p \quad (11)$$

$$\eta_{\text{cyc}} = \frac{W_{\text{net}}}{Q_e} \quad (12)$$

$$\eta_{\text{ove}} = \frac{W_{\text{net}} + Q_w}{Q_e} \quad (13)$$

$$\eta_{\text{ex}} = \frac{E_w + W_{\text{exp}} - W_p}{E_o} \quad (14)$$

$$E_w = \left(1 - \frac{T_{\text{amb}}}{T_{\text{ow}}}\right) Q_w \quad (15)$$

$$E_o = \left(1 - \frac{T_{\text{amb}}}{T_{\text{io}}}\right) Q_o \quad (16)$$

where Q_w is the heat absorbed by the cooling water; T_{amb} is the ambient temperature; T_{ow} is the temperature of the cooling water at the condenser outlet; E_w is the exergy of the cooling water; T_{io} is the temperature of the thermal oil at the evaporator inlet; Q_o is the heat released from the thermal oil; E_o is the exergy of the thermal oil.

2.5 Main routine flowchart of system

The flowchart of the overall simulation algorithm is shown in Fig. 5. Two parameters, T_e and T_d , are used to control the simulation processes. When the program is started, the assumed values of T_{d0} and T_{e0} will be assigned to those control parameters, respectively. Then, new T'_d and T'_e can be obtained by calling the subroutines of each part. If the deviations between those assumed values and iterated values are smaller than a given tolerance, the control parameters are identified, and the simulation results for each component can be outputted; otherwise, the iterated T'_d and T'_e replace the assumed T_{d0} and T_{e0} , and a new iteration will be repeated.

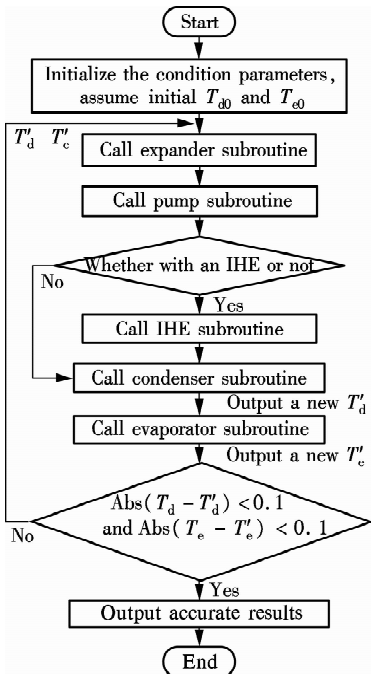


Fig. 5 Main routine flowchart of the ORC system

3 Simulation Results

Several graphs are plotted to show the influences of T_e and T_d on cycle efficiency, exergy efficiency and overall thermal efficiency, and the effects of the CHP technology and the IHE on the basic ORC system, with a fixed flow rate of cooling water and thermal oil.

3.1 Influences of heat source and heat sink temperatures on cycle performance

For a non-CHP ORC without IHE, the isentropic efficiency, work output and cycle efficiency vs. T_{io} are plotted in Fig. 6 at different condenser inlet temperatures of cooling water (T_{iw}).

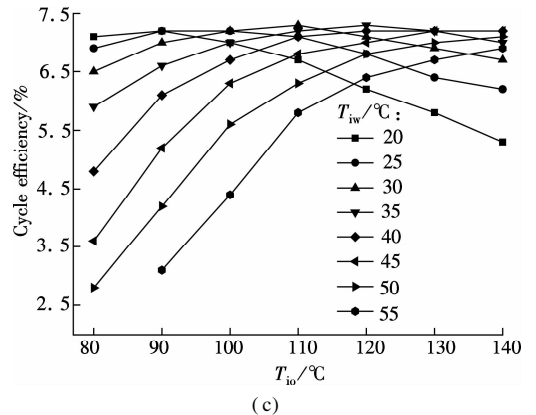
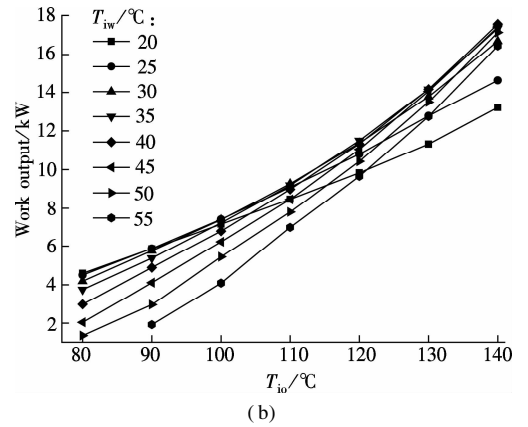
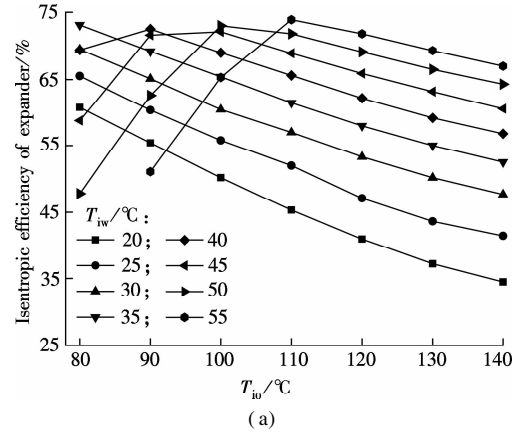


Fig. 6 Influences of T_{io} and T_{iw} on cycle performance.

(a) Isentropic efficiency; (b) Work output; (c) Cycle efficiency

For the selected scroll expander, its optimum isentropic efficiency appears when T_{iw} well matches T_{io} as shown in Fig. 6(a), and the cycle pressure ratio is about 2.5 under these conditions. As shown in Fig. 6(b), the work output increases with the increase of T_{io} . As shown in Fig. 6(c), when T_{iw} is less than 35 °C, the cycle efficiency increases first and then decreases as T_{io} increases. It is mainly because the isentropic efficiency decreases rapidly with the continuous increase of T_{io} . Thus, the increments in work output and cycle efficiency are limited. While the cycle efficiency increases but the growth rate decreases as T_{io} increases when T_{iw} is larger than 40 °C. The main reason is that the isentropic efficiency increases first and then decreases slowly.

In summary, for the selected scroll expander, a better temperature match between the heat source and heat sink leads to larger isentropic efficiency, work output and cycle efficiency. Moreover, the optimum cycle efficiencies, in the range of 7.0% to 7.3%, are obtained when the temperature differences between the heat source and the heat sink are in the range of 70 to 90 °C.

3.2 Influences of CHP technology

In order to improve the overall thermal efficiency and exergy efficiency, hot water can be obtained for the building by recycling the discharged heat in the condenser.

3.2.1 Influence of T_{io} and T_{iw} on T_{ow}

Since the temperature rise of cooling water is limited in the condenser, the lowest T_{iw} is required for obtaining hot water. The influences of T_{io} and T_{iw} on T_{ow} are shown in Fig. 7.

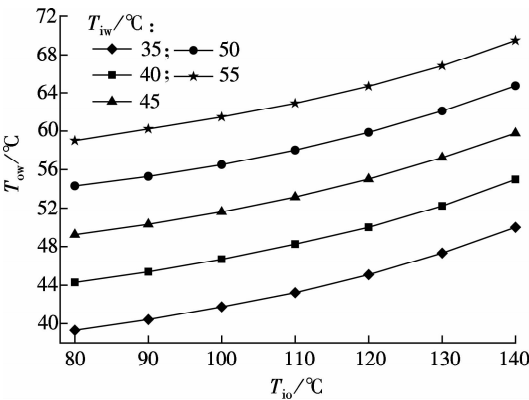


Fig. 7 Influences of T_{io} and T_{iw} on T_{ow}

It can be seen that T_{ow} increases as T_{io} increases. When T_{iw} is 35 °C, T_{ow} is less than 50 °C continuously with a fixed flow rate of cooling water, and water less than 50 °C cannot be used for domestic hot water. When T_{iw} is 40 °C, T_{ow} can meet the standard of domestic hot water only when T_{io} achieves 120 °C. Besides, the higher the T_{iw} , the lower the temperature requirement of the heat source. Therefore, to produce hot water, T_{iw} requires a minimum

value of 40 °C.

3.2.2 Influence of CHP technology on exergy and overall thermal efficiency

As is shown in Fig. 8(a), the exergy efficiency decreases as T_{iw} increases in the non-CHP ORC system. It is mainly because the higher the temperature, the greater the ambient heat loss, without consideration of heat recovery from cooling water. However, the exergy efficiency increases along with the increasing T_{iw} in the CHP ORC system, and it is 29% to 56% better than that in the non-CHP system. In addition, the overall thermal efficiency is equal to the cycle efficiency in the non-CHP system, but it reaches 90% or higher in the CHP system (see Fig. 8(b)). Therefore, the use of CHP technology will further improve the utilization rate of low-temperature heat sources. However, under actual conditions, the higher the temperature, the greater the heat loss; therefore, the overall thermal efficiency will decline.

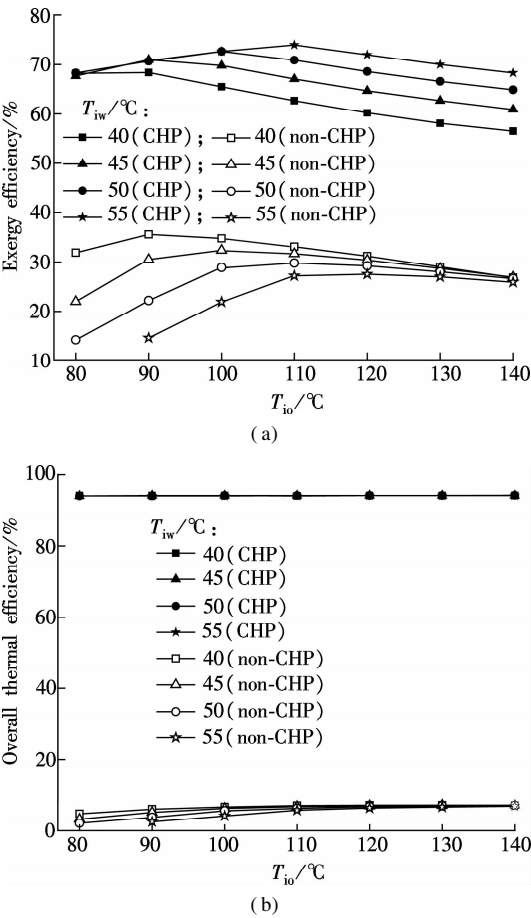


Fig. 8 Influence of CHP technology on efficiency. (a) Exergy efficiency; (b) Overall thermal efficiency

3.3 Influence of IHE on cycle indicators

For the CHP ORC systems with and without IHE, when T_{iw} is 45 °C, the cycle indicators vs. T_{io} are plotted in Fig. 9.

It can be seen from the simulation results that, as the heat source temperature increases, the trends of performance

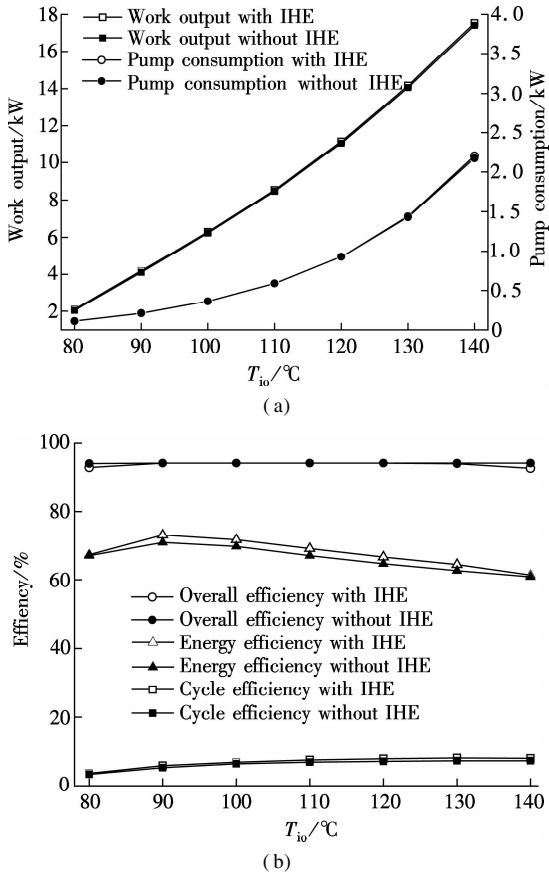


Fig. 9 Influence of IHE on cycle indicators. (a) Work output and pump consumption; (b) Cycle efficiency, exergy efficiency and overall thermal efficiency

curves remain unchanged by adding an IHE, and the performance improves somewhat. The work output in a cycle with an IHE is 0.06 to 0.13 kW larger than that without an IHE, and the growth of exergy efficiency and cycle efficiency are only about 1.3% and 0.6%, respectively. Therefore, from the simulation results under ideal condition, IHE has little effect on the improvement of the performance parameters of the CHP ORC system. Besides, based on heat loss, cost, complexity and other factors, IHE is not strongly recommended for an actual ORC plant.

4 Conclusions

1) For a non-CHP ORC without IHE, optimum cycle efficiency is related to the optimum pressure ratio. For the scroll expander selected in this paper, the optimum cycle efficiencies of 7.0% to 7.3% are obtained when the temperature difference between the heat source and the heat sink is in the range of 70 to 90 $^{\circ}\text{C}$.

2) For a CHP ORC, to produce hot water, the heat sink inlet temperature requires a minimum value of 40 $^{\circ}\text{C}$. In contrast to the non-CHP system, the use of the CHP technology will improve exergy efficiency and overall thermal efficiency by 29% to 56% and 87% to 90%, respectively.

3) The usage of the IHE will raise the exergy efficiency

and cycle efficiency of only about 1.3% and 0.6%, respectively. Therefore, IHE has little effect on the improvement of the efficiencies of the CHP ORC system. Besides, based on heat loss, cost, complexity and other factors, IHE is not strongly recommended for an actual ORC plant.

References

- [1] Manolakos D, Kosmadakis G, Kyritsis S. On site experimental evaluation of a low temperature solar organic Rankine cycle system for RO desalination[J]. *Solar Energy*, 2009, **83**(5): 646–656.
- [2] Madhawa H H D, Golubovic M, Worek W M, et al. Optimum design criteria for an organic Rankine cycle using low-temperature geothermal heat sources [J]. *Energy*, 2007, **32**(9): 1698–1706.
- [3] Liu H, Shao Y J, Li J X. A biomass-fired micro-scale CHP system with organic Rankine cycle (ORC)-thermodynamic modeling studies [J]. *Biomass and Bioenergy*, 2011, **35**(9): 3985–3994.
- [4] Wei D H, Lu X S, Lu Z, et al. Performance analysis and optimization of organic Rankine cycle (ORC) for waste heat recovery[J]. *Energy Conversion and Management*, 2007, **48**(4): 1113–1119.
- [5] Li M Q, Wang J F, He W F, et al. Construction and preliminary test of a low-temperature regenerative organic Rankine cycle (ORC) using R123 [J]. *Renewable Energy*, 2013, **57**(3): 216–222.
- [6] Jradi M, Li J X, Liu H, et al. Micro-scale ORC-based combined heat and power system using a novel scroll expander[J]. *International Journal of Low-Carbon Technologies*, 2014, **9**(2): 91–99.
- [7] Zheng N, Zhao L, Wang X D, et al. Experimental verification of a rolling-piston expander that applied for low-temperature organic Rankine cycle [J]. *Applied Energy*, 2013, **112**(16): 1265–1274.
- [8] Pei G, Li J, Li Y Z, et al. Construction and dynamic test of a small-scale organic Rankine cycle [J]. *Energy*, 2011, **36**(5): 3215–3223.
- [9] Qiu G Q. Selection of working fluids for micro-CHP systems with ORC [J]. *Renewable Energy*, 2012, **48**(6): 565–570.
- [10] Aghahosseini S, Dincer I. Comparative performance analysis of low-temperature organic Rankine cycle (ORC) using pure and zeotropic working fluids [J]. *Applied Thermal Engineering*, 2013, **54**(1): 35–42.
- [11] Saleh B, Koglbauer G, Wendland M, et al. Working fluids for low-temperature organic Rankine cycles [J]. *Energy*, 2007, **32**(7): 1210–1221.
- [12] Onkar Singh. *Applied thermodynamics* [M]. New Delhi, India: Mechanical Engineering Department, Harcourt Butler Technological Institute, 2009.
- [13] García-Cascales J R, Vera-García F, Corberán-Salvador J M, et al. Assessment of boiling and condensation heat transfer correlations in the modelling of plate heat exchangers [J]. *International Journal of Refrigeration*, 2007, **30**(6): 1029–1041.
- [14] Quoilin S. Sustainable energy conversion through the use of organic Rankine cycles for waste heat recovery and solar applications [D]. Liège, Belgium: University of Liège, 2011.

有机朗肯循环热电联产系统的模拟及性能分析

刘玉兰¹ 曹 政¹ 陈九法¹ 熊 健²

(¹ 东南大学能源与环境学院, 南京 210096)

(² 宝莲华新能源技术(上海)有限公司, 上海 200233)

摘要:为提高有机朗肯循环(ORC)的热效率,基于 RKS 状态方程编制模拟程序对热电联产系统进行模拟研究. 其中,循环工质选用 R245fa,涡旋膨胀机模型依据经验等熵膨胀效率建立,蒸发器和冷凝器选用板式换热器,并对单、两相区建立详细的传热模型. 该程序模拟了 7 个热源温度(80, 90, 100, 110, 120, 130, 140 ℃)和 8 个冷源温度(20, 25, 30, 35, 40, 45, 50, 55 ℃)下的循环工况. 结果表明:在无内热交换器 ORC 中,当冷热源温差处于 70 ~ 90 ℃,最佳循环效率为 7.0% ~ 7.3%;当冷源入口温度高于 40 ℃,CHP ORC 输出生活热水,且系统效率和热效率分别比非 CHP 系统增加了 29% ~ 56% 和 87% ~ 90%;内热交换器对 CHP ORC 系统输出功及效率的改善很小.

关键词:有机朗肯循环;热电联产;循环效率;效率;热效率

中图分类号:TK21